Journal of Molecular Spectroscopy 397 (2023) 111844

Contents lists available at ScienceDirect

Journal of Molecular Spectroscopy

journal homepage: www.elsevier.com/locate/yjmsp

Conformational analysis of carboxylic acid anhydrides: A microwave and computational study

Nathan Love [a], Aaron J. Reynolds [a], Michael A. Dvorak [b], Kenneth R. Leopold [a,*]

[a] Department of Chemistry, University of Minnesota, 207 Pleasant St., SE, Minneapolis, MN 55455, United States
[b] Department of Chemistry and Biochemistry, St. Cloud State University, 720 4th Ave. South, St. Cloud, MN 56301-4498, United States

ARTICLE INFO

Keywords:
Acid anhydrides
Microwave
Molecular structure
Molecular conformation
Supersonic jet
Computational chemistry

ABSTRACT

The microwave spectra of four carboxylic acid anhydrides, RCOOCOR′, (R,R′) = (CH_3, CF_3), ($C(CH_3)_3$, CF_3), (C_6H_5, CF_3) and (CH_3, $C(CH_3)_3$), have been observed in a supersonic jet. Calculations at the M06-2X/6-311++G(d,p) and MP2/6-311++G(d,p) levels of theory predict the lowest energy conformations for all four species to be nonplanar *cis* structures, i.e., conformations in which the C=O groups point in approximately the same direction, but are twisted out of a coplanar orientation. The observed spectra are consistent with these predictions. In addition, for all but the (R,R′) = (CH_3, $C(CH_3)_3$) species, higher energy nonplanar *trans* conformers are also predicted, typically within 1–2 kcal/mole the nonplanar *cis* form. For (R, R′) = ($C(CH_3)_3$, CF_3), extensive isotopic substitution has enabled a determination of most of the (non-fluorine) heavy atom structural parameters. Excellent agreement with the DFT and MP2 structures was obtained, thus validating the theoretical methods used. A strong correlation is found between the calculated O=C···C=O dihedral angle and the average of the vapor phase C=O stretching frequencies of RCOOH and R′COOH.

1. Introduction

Recent years have seen considerable interest in the structure and conformational complexity of flexible molecules in the gas phase [1–2]. While many types of systems have been studied, carboxylic acid anhydrides (RCOOCOR′) constitute a class that has received relatively limited attention [3]. Early studies of the simplest acid anhydride, formic anhydride, employed electron diffraction [4], microwave [5–6], and infrared techniques [7]. These works revealed only a single conformer in which the C=O bonds are in a *trans* configuration (i.e., pointing in roughly opposite directions). Although the original electron diffraction study indicated that the system is nonplanar, the subsequent investigations firmly established a planar geometry. The next most complex anhydride, formic acetic anhydride, has also been investigated in the gas phase by electron diffraction [8–9] as well as microwave [10] and infrared spectroscopy [9]. A normal coordinate analysis of condensed phase infrared and Raman spectra has also been reported [11]. Like formic anhydride, the system is planar (ignoring the out-of-plane CH_3 hydrogens) with a *trans* orientation of the carbonyl groups. Again, only a single conformer has been reported.

The planar geometries of formic and formic acetic anhydrides have been attributed to a strong intramolecular interaction between the formyl hydrogen and the carbonyl group adjacent to it [9]. Consistent with this picture, the accessible conformational landscape of acetic anhydride, which does not have a formyl hydrogen, is notably more complex. While early attempts to analyze the microwave spectrum of acetic anhydride, have proven elusive [10], the system was successfully studied in the gas phase by electron diffraction [12–13] and infrared spectroscopy [13]. Condensed phase vibrational spectra have also been analyzed [14]. In the electron diffraction work [13], two local minimum energy conformations were predicted by *ab initio* calculations, a *syn*-periplanar/*syn*-periplanar (sp,sp) and a *syn*-periplanar/anti-clinal (sp, ac), which can alternatively be described as nonplanar *cis* and nonplanar *trans* respectively. (Note, again, that the use of the term planar ignores out-of-plane CH_3 hydrogens and refers, instead, to the O=C–O–C=O plane.) A dynamical model incorporating both local minima and a grid of intermediate structures between them was able to reproduce the room temperature IR spectra and the electron diffraction results. Maleic [15], phthalic [16–17], and succinic [18] anhydrides have also been studied in the gas phase, and share the common feature that the two carbonyl groups are locked into a coplanar arrangement of the carbonyl groups by the ring structure of the molecule.

* Corresponding author.
E-mail address: kleopold@umn.edu (K.R. Leopold).

https://doi.org/10.1016/j.jms.2023.111844
Received 1 August 2023; Received in revised form 12 October 2023; Accepted 14 October 2023
Available online 16 October 2023

Two additional carboxylic anhydrides have recently been studied in our laboratory: trifluoroacetic anhydride [19] and pivalic anhydride [20]. Both have been observed in the nonplanar *cis* conformation with no indication of other forms. In this work, we present a microwave and computational study of four additional carboxylic acid anhydrides for which the lowest energy conformer is predicted to have a nonplanar *cis* arrangement of the two carbonyl groups: RCOOCOR′, (R,R′) = (CH_3, CF_3), ($C(CH_3)_3$, CF_3), (C_6H_5, CF_3), and (CH_3, $C(CH_3)_3$). Table 1 summarizes the names and abbreviations used in this work for these systems, and also includes the trifluoroacetic [19] and pivalic anhydrides [20] previously studied. The new results are combined with those of the prior work and are used to explore the influence of R groups on the dihedral angle formed by the two C=O groups. We note that, as described below for some of these systems, *trans* conformations are also predicted to be local minima on the potential energy surface, and that additional microwave work in our laboratory has indicated *trans* configurations for both acetic and acetic difluoroacetic anhydrides, (R,R′) = (CH_3, CH_3) and (CH_3, CF_2H), respectively [21]. In this paper, however, we focus only on systems for which the lowest energy form is *cis*.

2. Experimental methods and results

The anhydrides studied in this work were not commercially available and required synthesis. Several methods for the preparation of mixed carboxylic anhydrides exist in the literature [22–24] but the procedure associated with the reaction depicted in equation 1 [23] was used.

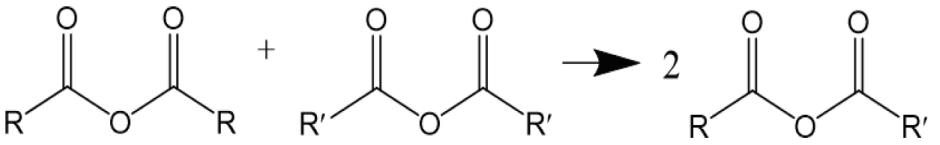

(1)

This scheme was chosen because of its 100 % atom economy and lack of need for further distillation or purification (assuming the reaction is kept dry and goes to completion). Batches were prepared using approximately 50 mmol of each reagent. The post-reaction mixtures were observed as clear, pale-yellow liquids. Additional details are provided in the Supplementary Material.

Supersonic jet microwave spectra of each anhydride were measured with our tandem chirped-pulse and cavity microwave spectrometer [25–26]. The anhydrides were introduced to the system by flowing argon at a pressure of approximately 0.5 atm over a 1.5 mL sample stored in a stainless-steel reservoir. The reservoir was gently heated to between 50 and 70 °C for BzTFAA and APiA. The resulting mixture of argon and anhydride vapors was then flowed through a 0.016 in. inner diameter needle along the axis of a stainless-steel cone nozzle through which argon was simultaneously pulsed at a stagnation pressure of ~ 1.0 atm to create the supersonic expansion. Following the acquisition of chirped-pulse data, additional scans with the cavity system were conducted to resolve dense regions of broadband spectra. Typical uncertainties in the measured frequencies are 10 kHz and 2 kHz for the chirped pulse and cavity spectrometers, respectively. Assigned transitions with labelled torsional states, where appropriate, can be found in the Supplementary Material for all four anhydrides studied.

Table 1
Summary of Names and Abbreviations for the Anhydrides Disucssed in This Work.

Name	R	R′	Abbreviation
Trifluoroacetic Anhydride	CF_3	CF_3	TFAA
Acetic Trifluoroacetic Anhydride	CH_3	CF_3	ATFAA
Pivalic Trifluoroacetic Anhydride	$C(CH_3)_3$	CF_3	PiTFAA
Benzoic Trifluoroacetic Anhydride	C_6H_5	CF_3	BzTFAA
Acetic Pivalic Anhydride	CH_3	$C(CH_3)_3$	APiA
Pivalic Anhydride	$C(CH_3)_3$	$C(CH_3)_3$	PiA

2.1. Systems with no CH_3 internal rotation

Transitions of PiTFAA and BzTFAA were assigned using the DAPPERS package [20]. The spectra were fit to semi-rigid rotor Watson A-reduced Hamiltonian in the I^r representation using Pickett's SPFIT [27] program, as accessed through the DAPPERS interface. For PiTFAA, transitions of the singly substituted ^{13}C isotopologues were measured in natural abundance for all carbon atoms. Two of the singly substituted carbonyl ^{18}O isotopologues were also observed but no measurements were made involving substitution on the bridging oxygen, which was determined to be too close to the center of mass to provide any meaningful information. For BzTFAA, only two isotopologues, the parent and $^{13}C4$ (see Fig. 1 for atom numbering), were observed due to lower signal intensity, but the ^{13}C isotope shift was found to be well predicted by the theoretical structure described below. Values of J and K_p included in the fits were between $J" = 2$ and 25 and $K_p" = 0$ to 14 for PiTFAA and between $J" = 2$ and 36 and $K_p = 0$ and 14 for BzTFAA. Only *a*- and *b*-type transitions were observed for both species. Fitted spectroscopic constants for the parent forms are given in Tables 2 and 3 and compared with theoretical values (see below). Tables 4 and 5 present the fitted spectroscopic constants for all isotopologues observed. A portion of the PiTFAA chirped-pulse spectrum is shown in Fig. 2 and a sample cavity spectrum is shown in Fig. 3.

2.2. Systems with a CH_3 internal rotor

For ATFAA and APiA, (i.e. the two anhydrides of the form $CH_3COOCOR'$), the rigid rotor-like spectra of the A states were assigned and fit and the resulting constants were combined with the theoretical internal rotor parameters (described below) to produce a simulated spectrum that was highly predictive of the remaining E state transitions. The two states were then fit together with XIAM [28] using rotational and quartic distortion parameters as well as the internal rotation barrier, V_3, the rotor polar angles, δ and ε, and internal rotation distortion parameters. The polar angles are particularly pertinent to the discussion below and are defined as follows: δ is the angle between the CH_3 top axis and the *a*-axis of the molecule, and ε is the angle between the *b*-axis of the molecule and the projection of the top axis onto the *b*-*c* plane. The fitted parameters for ATFAA and APiA are shown in Tables 6 and 7 respectively. Relative strengths of the observed *a*-, *b*-, and *c*-type transitions are also indicated in the tables.

2.3. Isotopic substitution data

The heavy atom structure of PiTFAA was determined via a Kraitchman analysis [29], as implemented using Kisiel's KRA program [30]. The resulting atomic coordinates are included in the Table 8, where the Costain uncertainties, described in the KRA documentation, are

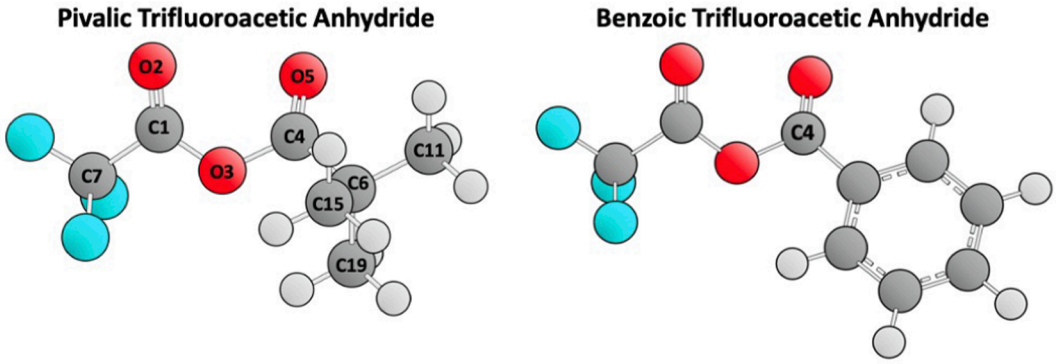

Fig. 1. The structure of pivalic trifluoroacetic anhydride and benzoic trifluoroacetic anhydride determined with M06-2X/6-311++G(d,p) calculations. Atoms for which ^{13}C and ^{18}O isotopologue spectra were observed have been labelled with the exception of O3 in pivalic trifluoroacetic anhydride which was not observed due to proximity to the principal axis system origin. Only one isotopologue of benzoic trifluoroacetic anhydride (^{13}C4) was pursued. Both species are shown in the nonplanar *cis* conformation, which is the lowest energy structure.

Table 2
Fitted and Computed Spectroscopic Constants of Parent Pivalic Trifluoroacetic Anhydride and Comparison with Theoretical Values.

		***cis* Conformer**[a]	
	Experimental	**M06-2X**[b]	**MP2**[b]
A [MHz]	1579.471847(33)	1576	1577
B [MHz]	441.570027(19)	445	442
C [MHz]	413.612330(17)	413	415
Δ_J [kHz]	0.015313(43)		
Δ_{JK} [kHz]	0.15106(24)		
Δ_K [kHz]	0.01691(93)		
δ_J [kHz]	0.000179(17)		
δ_K [kHz]	0.1561(62)		
$\lvert\mu_a\rvert$ [D]	Strong	3.1	3.1
$\lvert\mu_b\rvert$ [D]	Strong	2.7	2.3
$\lvert\mu_c\rvert$ [D]	-	0.5	0.5
N [c]	509 (405)		
RMS [kHz]	3.4		

(a) No potential minimum near a *trans* configuration was found at the level of theory employed.
(b) Calculations employed the 6-311++G(d,p) basis set.
(c) Number of assigned transitions in the fit. Number in parentheses denotes number of distinct frequencies in the fit.

reported. Atom numbering is given in Fig. 1 and the signs of the atomic coordinates were inferred based on the theoretical calculations presented below. Bond lengths, bond angles, and dihedral angles derived from these coordinates are shown in Table 9 along with a comparison to computational values from the M06-2X/6-311++G(d,p) and MP2/6-311++G(d,p) calculations. Agreement is seen to be quite good, typically a few hundredths of an angstrom for distances and a few degrees for angles. As noted above, only one ^{13}C isotopologue was observed for BzTFAA (C4), and its spectra were well predicted by the computed structure. These results validate the levels of theory used in

Table 3
Fitted and Computed Spectroscopic Constants of Parent Benzoic Trifluoroacetic Anhydride and Comparison with Theoretical Values.

		M06-2X[a]		**MP2**[a]	
	Experimental	***cis***	***trans***	***cis***	***trans***
A [MHz]	1450.101414(68)	1443	1539	1444	1503
B [MHz]	299.142841(10)	302	317	299	315
C [MHz]	266.407241(14)	267	301	267	304
Δ_J [kHz]	0.007362(18)				
Δ_{JK} [kHz]	0.01494(23)				
Δ_K [kHz]	0.5192(16)				
δ_J [kHz]	0.0019020(93)				
δ_K [kHz]	−0.0403(17)				
N [b]	516 (432)				
RMS [kHz]	4.1				
$\lvert\mu_a\rvert$ [D]	Strong	4.3	4.8	4.1	4.5
$\lvert\mu_b\rvert$ [D]	Strong	2.6	0.5	2.2	0.8
$\lvert\mu_c\rvert$ [D]	–	0.1	1.4	0.1	1.3
Relative Energy[c]	–	0	1.52(1.59)	0	2.05(2.16)

(a) Calculations employed the 6-311++G(d,p) basis set.
(b) Number of assigned transitions in the fit. Number in parentheses denotes number of distinct frequencies in the fit.
(c) All energies are in kcal/mol. Values in parentheses are zero-point corrected. Uncorrected energies are relative to the most stable conformer calculated at the same level of theory. Zero-point corrected energies are relative to the form that has the lowest zero-point corrected energy.

Table 4
Fitted Spectroscopic Constants for all Pivalic Trifluoroacetic Anhydride Isotopologues[a,b].

	Parent	^{13}C1	^{18}O2	^{13}C4	^{18}O5
A [MHz]	1579.471847(33)	1577.5276(14)	1547.5540(37)	1577.5114(12)	1547.9550(76)
B [MHz]	441.570027(19)	441.214408(75)	440.40123(16)	440.834004(69)	439.59609(37)
C [MHz]	413.612330(17)	413.216050(80)	411.12198(22)	412.898937(66)	410.49618(39)
Δ_J [kHz]	0.015313(43)	0.01479(49)	0.0120(14)	0.01572(41)	0.0153(31)
Δ_{JK} [kHz]	0.15106(24)	0.1521(18)	0.163(24)	0.1507(26)	0.148(52)
Δ_K [kHz]	0.01691(93)	[0.01691]	[0.01691]	[0.01691]	[0.01691]
δ_J [kHz]	0.000179(17)	[0.000179]	[0.000179]	[0.000179]	[0.000179]
δ_K [kHz]	0.1561(62)	[0.1561]	[0.1561]	[0.1561]	[0.1561]
N [c]	509 (405)	23	12	24 (22)	11
RMS [kHz]	3.4	0.8	2.4	1.0	1.8
	^{13}C6	^{13}C7	^{13}C11	^{13}C15	^{13}C19
A [MHz]	1578.91835(88)	1579.2585(18)	1578.4910(20)	1565.2244(29)	1563.7159(11)
B [MHz]	439.15065(11)	439.682640(85)	435.98533(18)	438.40141(20)	439.10238(10)
C [MHz]	411.45017(10)	411.941731(95)	408.67345(17)	411.55067(14)	410.65979(11)
Δ_J [kHz]	0.01536(48)	0.01513(53)	0.01455(81)	0.0147(10)	0.01419(42)
Δ_{JK} [kHz]	0.1596(59)	0.1426(32)	0.1485(38)	0.170(17)	0.1491(29)
Δ_K [kHz]	[0.01691]	[0.01691]	[0.01691]	[0.01691]	[0.01691]
δ_J [kHz]	[0.000179]	[0.000179]	[0.000179]	[0.000179]	[0.000179]
δ_K [kHz]	0.162(41)	[0.1561]	0.195(69)	[0.1561]	0.172(4)
N[c]	19	21	23	18	22
RMS [kHz]	0.6	1.1	1.4	2.1	0.8

(a) Atom numbering is given in Fig. 1.
(b) Numbers in square brackets were constrained to parent values.
(c) Number of assigned transitions in the fit. Number in parentheses denotes number of distinct frequencies in the fit if different from *N*.

Table 5
Fitted Spectroscopic Constants for both Benzoic Trifluoroacetic Anhydride Isotopologues[a,b].

	Parent	^{13}C4
A [MHz]	1450.101414(68)	1446.1135(29)
B [MHz]	299.142841(10)	299.07098(26)
C [MHz]	266.407241(14)	266.22315(11)
Δ_J [kHz]	0.007362(18)	0.00790(41)
Δ_{JK} [kHz]	0.01494(23)	[0.01494]
Δ_K [kHz]	0.5192(16)	[0.5192]
δ_J [kHz]	0.0019020(93)	0.00237(33)
δ_K [kHz]	−0.0403(17)	[-0.0403]
N [c]	516 (432)	20
RMS [kHz]	4.1	1.3

(a) Atom numbering is given in Fig. 1.
(b) Numbers in square brackets were constrained to parent values.
(c) Number in parenthesis denotes the number of distinct frequencies in the fit if different from *N*.

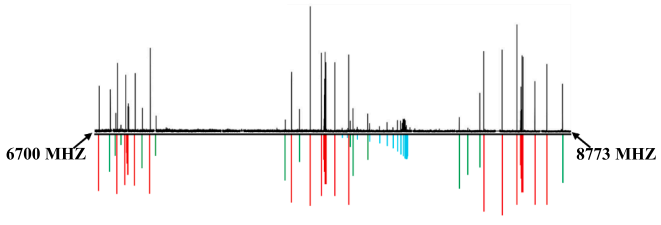

Fig. 2. A portion of the PiTFAA chirped-pulse spectrum between 6700 and 8733 MHz showing three *J* clusters of transitions. The below spectrum is the fitted simulated spectrum. Red transitions are R branch *a*-type, green transitions are R branch *b*-type, and teal transitions are Q branch *b*-type.

this work and extensive isotopic substitution was not pursued for the remaining systems studied.

3. Computational methods and results

Minimum energy structures of all four mixed carboxylic anhydrides were located with M06-2X/6-311++G(d,p) and MP2/6-311++G(d,p) calculations using the Gaussian16 suite of programs [31]. All structures were checked for the absence of imaginary frequencies, and zero-point corrected energies were also obtained. The calculated global minimum energy structure was determined to be a nonplanar *cis* configuration for all four systems studied. (This is the configuration depicted in Fig. 1.) In addition, calculations for TFAA and PiA were performed at the M06-2X/6-311++G(d,p) and MP2/6-311++G(d,p) levels of theory. The nonplanar *cis* conformers of these systems, which represent their global potential energy minima, have been previously investigated, both experimentally and computationally [19,20]. However, the computations employed a slightly different basis set and thus new calculations using the 6-311++G(d,p) basis set enable these systems to be included in valid comparisons with the anhydrides reported here. Cartesian coordinates for all minimum energy structures are given in the Supporting Information. For systems containing a methyl rotor (ATFAA and APiA), internal rotation barriers, V_3, were obtained by locating a transition state along the CH_3 internal rotation coordinate. Calculated rotational constants and dipole moment components are given in Tables 2, 3, 6, and 7. For systems with methyl group internal rotation, calculated values of V_3 and the polar angles δ and ε are also included (Tables 6 and 7).

In addition to the nonplanar *cis* global minima, local minima in a nonplanar *trans* configuration were identified for all systems studied with the exception of PiTFAA. In that case, attempts to locate a *trans* form converged on the nonplanar *cis* structure. For the other systems, however, the *trans* conformers appeared and were typically within 2 kcal/mol of the global energy minimum, depending on the R groups and the method of calculation. Interestingly, attempts to locate transition states along the CH_3 internal rotation coordinate did not converge, prompting more careful examination of the calculated electronic energy as a function of the CH_3 internal rotation angle. These calculations revealed irregularities in the three-fold potential which appeared either as inflections or an additional minimum located about 30 degrees away from the deepest *trans* minimum. These results are shown in Fig. 4, which was generated by stepping the CH_3 internal rotation angle and optimizing all other structural parameters. It may be seen from the figure that the MP2 calculations give the lowest energy *trans* configurations at an angle of approximately 120 degrees for both anhydrides while the M06-2X calculations place it slightly above 90 degrees. The corresponding structures and the definition of these angles are shown in the inset and the two structures are designated $trans^{120}$ and $trans^{90}$,

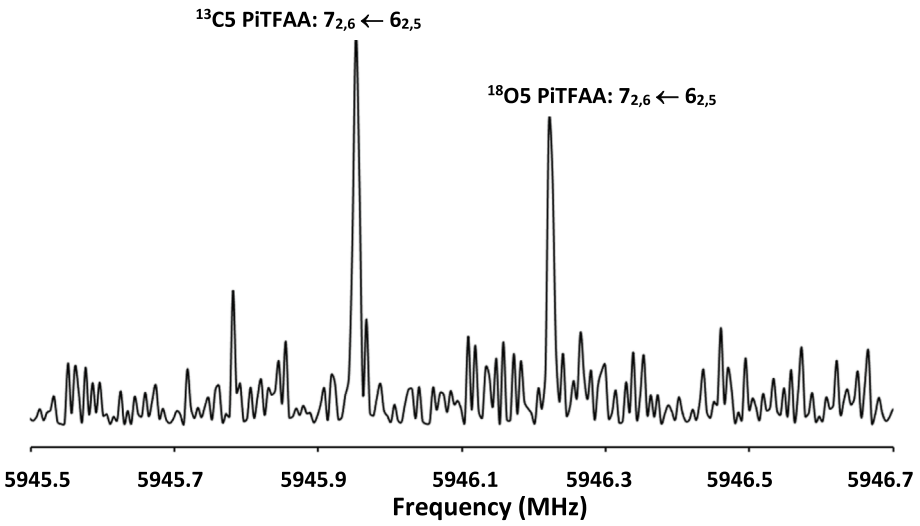

Fig. 3. A portion of the cavity spectrum of PiTFAA. This particular segment includes transitions from both ^{18}O5 and ^{13}C15 PiTFAA isotopologues.

Table 6
Fitted and Computed Spectroscopic Constants for Acetic Trifluoroacetic Anhydride and Comparison with Theoretical Results.

		M06-2X[a]			MP2[a]	
		cis	*trans*^{90}	*trans*^{120}	*cis*	*trans*^{120}
A [MHz]	2648.74070(26)	2651	2677	2692	2626	2673
B [MHz]	817.827036(76)	824	818	800	817	788
C [MHz]	737.724205(73)	738	740	764	740	776
Δ_J [kHz]	0.05513(28)					
Δ_{JK} [kHz]	0.35033(97)					
Δ_K [kHz]	0.0769(47)					
δ_J [kHz]	0.00048(13)					
F_o [GHz]	[158.1][b]	158.1	158.3	157.8	157.6	157.3
V_3 [cm^{-1}]	326.610(94)	311	273	273	324	286
ε [deg]	22.003(62)	21	24	34	25	70
δ [deg]	129.933(57)	128	108	109	128	140
$D_{\pi 2K}$ [MHz]	−0.016(56)					
$D_{\pi 2}$ [MHz]	−0.0206(14)					
N[c]	290					
RMS [kHz]	4.1					
$\lvert\mu_a\rvert$ [D]	Strong	2.2	1.3	1.6	2.3	1.8
$\lvert\mu_b\rvert$ [D]	Strong	3.1	1.8	1.4	2.7	1.2
$\lvert\mu_c\rvert$ [D]	Weak	0.8	1.5	2.2	0.8	2.3
Rel. Energy	–	0	0.80 (0.91)	0.86 (0.86)	0	0.92 (0.87)

(a) All energies are in kcal/mol and were obtained using the 6-311++G(d,p) basis set. Values in parentheses are zero-point corrected. Uncorrected energies are relative to the most stable conformer calculated at the same level of theory. Zero-point corrected energies are relative to the form that has the lowest zero-point corrected energy. The calculated constants listed under "*trans*^{90}" and "*trans*^{120}" refer to those calculated for the local minimum energy structures at CH_3 internal rotation angles of 90 and 120 degrees, respectively (See Fig. 4).
(b) Theoretical value, constrained in fit.
(c) Number of transitions in the fit.

respectively. Careful examination of the Cartesian coordinates for APiA suggest that these irregularities may arise from a weak intramolecular interaction between one of the methyl hydrogens and the oxygen of the remote carbonyl, i.e., the carbonyl on the other side of the bridging oxygen. (The shortest H···O distances are 2.55 Å and 2.59 Å for the 90 degree and 120 degree structures, respectively, with slightly different configurations of the heavy atom frame.) However, while such an interaction seems entirely plausible, the differences between the M06-2X and MP2 results render it unclear as to whether it causes an inflection or a genuine minimum in the potential energy surface. Moreover, even if a secondary minimum is real, it is unclear as to whether it is relevant to the vibrationally averaged structure of the *trans* conformer. Further examination of these questions was not pursued, however, as this work is focused primarily on the global (*cis*) minimum energy configurations. The *cis* configurations do not show these irregularities, as the CH_3 group is far from the remote carbonyl (see Fig. 1).

4. Discussion

In this section, we compare the experimental evidence with the theoretical predictions in order to establish that the *cis* forms were, indeed, the ones observed. We then discuss trends in the calculated degree of out-of-plane twisting, as measured by the dihedral angle between the two carbonyl groups. As noted above, because of the low temperature of the supersonic jet, it is likely that the observed conformer is the lowest energy form.

4.1. Comparison between theory and experiment – assignment to the cis conformation

4.1.1. PiTFAA

Comparison between the experimental and theoretical rotational constants in Table 2 show excellent agreement and confirm the

Table 7
Fitted and Computed Spectroscopic Constants for Acetic Pivalic Anhydride and Comparison with Theoretical Results.

		M06-2X[a]		MP2[a]		
		cis	*trans*^{90}	*cis*	*trans*^{90}	*trans*^{120}
A [MHz]	2398.50253(28)	2415	2428	2398	2420	2429
B [MHz]	845.01595(17)	848	843	844	836	818
C [MHz]	786.23188(20)	788	761	782	769	796
Δ_J [kHz]	0.19103(67)					
Δ_{JK} [kHz]	0.3427(58)					
Δ_K [kHz]	0.1693(62)					
δ_J [kHz]	−0.02605(30)					
δ_K [kHz]	0.201(55)					
F_o[GHz]	[160.0][b]	159.9	158.5	159.1	158.1	157.4
V_3 [cm^{-1}]	268.569(33)	247	278	240	177	177
ε [deg]	152.484(39)	150	157	151	154	146
δ [deg]	138.783(30)	137	108	136	106	110
$D_{\pi 2J}$ [MHz]	−0.14592(85)					
$D_{\pi 2K}$ [MHz]	0.3712(32)					
N[c]	105					
RMS [kHz]	4.1					
$\lvert\mu_a\rvert$ [D]	Weak	0.7	2.1	0.7	1.9	1.4
$\lvert\mu_b\rvert$ [D]	Strong	3.7	0.9	3.4	0.8	0.8
$\lvert\mu_c\rvert$ [D]	Weak	0.3	1.8	0.2	2.0	2.7
Rel. Energy[b]	–	0.19 (−0.04)	0	0	0.84 (1.00)	0.77 (0.76)

(a) All energies are in kcal/mol and were obtained using the 6-311++G(d,p) basis set. Values in parentheses are zero-point corrected. Uncorrected energies are relative to the most stable conformer calculated at the same level of theory. Zero-point corrected energies are relative to the form that has the lowest zero-point corrected energy. In cases where *trans*^{90} and *trans*^{120} minima are predicted, the energy given is that of the lower energy structure. A negative sign indicates that the energy ordering of the conformers inverts after zero-point correction. The calculated constants listed under "*trans*^{90}" and "*trans*^{120}" refer to those calculated for the local minimum energy structures at CH_3 internal rotation angles of 90 and 120 degrees, respectively (See Fig. 4).
(b) Theoretical value, constrained in fit.
(c) Number of transitions in the fit.

Table 8
Experimental Coordinates for Pivalic Trifluoracetic Anhydride[a].

	a [Å]	*b* [Å]	*c* [Å]
C1	−0.9235(16)	0.5684(27)	0.2705(56)
O2	−0.9819(15)	1.65559(91)	0.7792(19)
C4	1.3485(11)	0.5481(28)	−0.3157(48)
O5	1.4085(11)	1.63307(92)	−0.8039(19)
C6	2.51610(60)	−0.3394(45)	0.0414*i*[b]
C7	−2.22066(68)	−0.2078(73)	−0.022(69)
C11	3.82982(40)	0.3945(39)	−0.2177(70)
C15	2.39663(63)	−0.6101(25)	1.60327(94)
C19	2.44878(62)	−1.67448(91)	−0.6752(23)

(a) Signs are inferred from the theoretical structure. Atom numberings refer to Fig. 1.
(b) Imaginary coordinate.

Table 9
Structural Parameters for Pivalic Trifluoroacetic Anhydride[a].

Bond Lengths [Å]	**Experimental**	**M06-2X**	**MP2**
C1-O2	1.2017(36)	1.182	1.198
C4-O5	1.1913(34)	1.182	1.194
C1-C7	1.540(14)	1.545	1.543
C4-C6	1.5002(84)	1.513	1.509
C6-C11	1.5205(61)	1.528	1.529
C6-C15	1.630(36)	1.538	1.539
C6-C19	1.498(17)	1.537	1.538
Bond Angles [deg]			
O2-C1-C7	119.7(10)	123.5	124.1
O5-C4-C6	125.86(53)	128.8	129.2
C4-C6-C11	110.90(78)	108.2	108.5
C4-C6-C15	104.4(14)	108.2	108.1
C4-C6-C19	113.4(14)	109.0	109.3
C11-C6-C15	106.5(16)	110.7	110.4
C11-C6-C19	113.9(13)	110.7	110.5
C15-C6-C19	107.0(11)	110.0	110.0
Dihedral Angles [deg]			
O2-C1-C4-O5	46.61(39)	43.0	50.3
O5-C4-C6-C11	7.4(29)	0.6	1.8
O5-C4-C6-C15	121.70(75)	119.3	118.0
O5-C4-C6-C19	122.23(85)	121.0	122.3

(a) Atom numberings refer to Fig. 1. The imaginary *c*-coordinate of C6 is. taken to be zero in calculating these values.

nonplanar *cis* geometry. Moreover, the experimental structural parameters in Table 9 are in excellent agreement with the values calculated by both theoretical methods employed, providing a strong measure of confidence in both the assignment to the *cis* form and in the level of theory used in these studies. As noted in the previous section, only a *cis* conformer was found computationally for this system.

4.1.2. BzTFAA

For benzoic trifluoroacetic anhydride, potential energy minima at both nonplanar *cis* and nonplanar *trans* geometries were located. A comparison of the experimental and theoretical rotational constants in Table 3 decisively favors assignment to the *cis* conformer, and the absence of observable *c*-type transitions is only compatible with the computed dipole moment components for that form. This assignment is consistent with the predicted energy ordering.

4.1.3. ATFAA

Both *cis* and *trans* conformers were predicted for acetic trifluoroacetic anhydride as shown in Table 6, with the nonplanar *cis* form predicted by both the M06-2X and MP2 methods to be the global minimum by over 0.8 kcal/mol. Overall, the rotational constants from both the M06-2X and MP2 calculations show better agreement with experiment for the *cis* form, with the exception of the *B* constant obtained at the M06-2X level for the *trans*^{90} minimum. However, neither calculation for the *cis* or *trans*^{90} minimum disagrees egregiously with the observed value. The predicted polar angle ε is in best agreement for the *cis* form with both the M06-2X and MP2 methods, though the agreement for the two *trans* conformers predicted at the M06-2X level are not unreasonable and the better agreement with the *cis* form may be fortuitous. For both methods, however, the predicted values of δ show a clear preference for

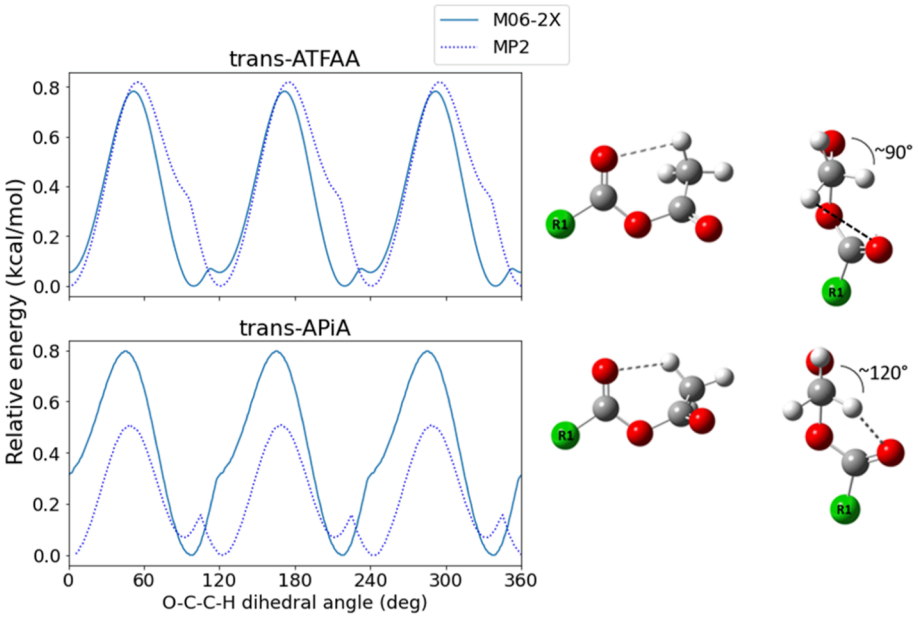

Fig. 4. M06-2X/6-311++(d,p) and MP2/6-311++(d,p) energies as a function of the CH_3 internal rotation angle for acetic trifluoroacetic and acetic pivalic anhydrides in the vicinity of the local minimum energy structure (i.e., the nonplanar *trans* configuration). The step size is 1 degree, with the internal rotation angle fixed and all other structural parameters optimized. The zero of energy on the plots is the lowest energy calculated for a 360° internal rotation of the CH_3 group in the *trans* configuration of the anhydride. The right side of the figure shows views of the local minima designated as $trans^{90}$ and $trans^{120}$ degrees on the plots.

Table 10
Theoretical Carbonyl Dihedral Angles in NonPlanar *cis* Anhydrides and Vibrational Frequencies of the Parent Acids.

R	R′	ν(C=O)[a] (cm^{-1})	ν'(C=O)[a] (cm^{-1})	Average C=O Stretching Frequency[b]	O=C···C=O Dihedral Angle (deg)[c] M06-2X	O=C···C=O Dihedral Angle (deg)[c] MP2
CF_3	CF_3	1830	1830	1830	32.6	40.1
CF_3	CH_3	1830	1799	1815	39.5	44.6
CF_3	C_6H_5	1830	1752	1791	40.4	47.5
CF_3	$C(CH_3)_3$	1830	1774	1802	43.0	50.3
CH_3	$C(CH_3)_3$	1799	1774	1787	56.2	54.9
$C(CH_3)_3$	$C(CH_3)_3$	1774	1774	1774	57.8	57.0

(a) ν and ν' are the experimental vapor-phase stretching frequencies for RCOOH and R′COOH, respectively. Gas phase vibrational frequencies are taken from reference [32] for CF_3COOH, [33] for C_6H_5COOH, [34] for $(CH_3)_3CCOOH$, and [35] for CH_3COOH.
(b) Average of ν(C=O) and ν'(C=O).
(c) Calculated dihedral angle in the anhydride derived from R and R′.

the *cis* conformation. Similarly, the experimental V_3 barriers are in better agreement with those calculated for the *cis* conformer. Finally, strong *a*- and *b*-type spectra and a weak *c*-type spectrum were observed which is only consistent with the predicted dipole moment components of the nonplanar *cis* form. Thus, taken collectively, we assign the observed spectrum to the *cis* conformer.

4.1.4. APiA

As seen in Table 7 for acetic pivalic anhydride, the MP2 calculations without zero-point energy corrections place either *trans* form 0.7 – 1.0 kcal/mole higher in energy than the *cis* configuration, while those using the M06-2X method predict a $trans^{90}$ form to be 0.2 kcal/mol lower in energy. However, after zero-point corrections, the M06-2X calculations predict the *cis* and *trans* forms to be essentially isoenergetic, while the MP2 calculations retain the *cis* < *trans* energy ordering. Comparison with the experimental rotational constants reveals better agreement with the *cis* form calculated by either of the theoretical methods. The computed V_3 barrier for the $trans^{90}$ form is in somewhat better agreement with experiment than that obtained for the *cis* form from the M06-2X calculations, though neither is egregiously in error. With the MP2 method, however, the calculated barrier clearly favors the *cis* conformer. At either level of theory, the predicted values of ε agree reasonably well with the experimental result and therefore do not provide useful information. However, for both the MP2 and M06-2X calculations, the polar angle, δ, is in much better agreement with fitted value for the *cis* conformer. Finally, the strong observed *b*-type spectrum is only compatible with the predicted dipole moments of the nonplanar *cis* conformation. Thus, the preponderance of evidence indicates that the *cis* conformer was the one observed.

4.2. Correlation with free acid C=O stretching frequencies

The majority of carboxylic anhydrides studied by microwave spectroscopy, including four reported in this study, have been observed in the nonplanar *cis* conformation. However, the C=O dihedral angles vary considerably, and it is of interest to try to understand these variations. One obvious starting point involves consideration of the effect of R groups with differing electronic character on the nature of the carbonyl moiety. The carbonyl stretching frequency in the gas phase free acid provides one measure of this. Table 10 gives the experimental vapor-phase C=O stretching frequencies for the free acids and the dihedral angles calculated by both theoretical methods employed in this work [32–35]. Inasmuch as the dihedral angle in the anhydride involves both carbonyl groups, Fig. 5 displays a plot of the average of the C=O stretching frequencies for RCOOH and R′COOH vs. the calculated dihedral angle. For this purpose, the average of the angles obtained from

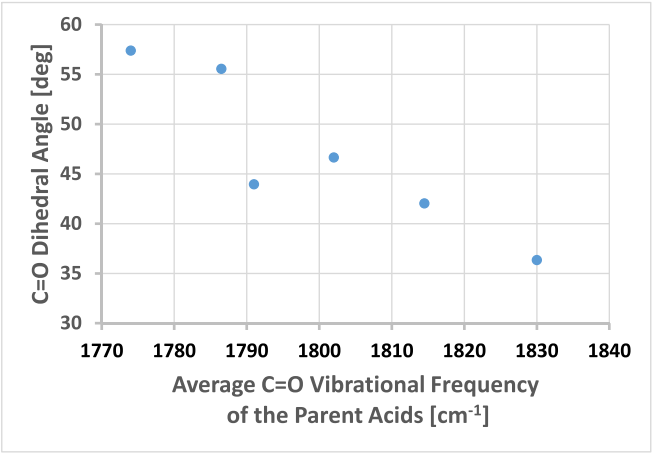

Fig. 5. Plot of the average of the calculated O=C—C=O dihedral angles in the *cis* conformers of the anhydrides formed from RCOOH and R′COOH vs. the average of the experimental vapor phase C=O stretching frequencies in RCOOH and R′COOH. The calculated dihedral angles are the average values obtained from M06-2X and MP2 calculations with the 6-311++G(d,p) basis set. Data for the plot are given in Table 10. The point that falls off the curve corresponds to BzTFAA.

the M06-2X and MP2 calculations are used, though separate plots using results of either method look the same. It may be seen from the figure that the dihedral angle in the anhydride is strongly correlated with the average stretching frequency of the parent acids. Note that separate M06-2X/6-311++G(d,p) calculations of the symmetric and antisymmetric stretching frequencies of the anhydrides show the same trend.

The correlation shown in Fig. 5 is empirical, and it is of interest to attempt to read some physical interpretation into it. The simplest and most chemically intuitive explanation involves mutual repulsion of the carbonyl oxygens which is expected to increase with increasing negative charge on the oxygens. Naively, to the extent that the C=O bond is weakened, an increased negative charge would correlate with an increasing contribution of a $C^{+}-O^{-}$ resonance structure. Thus, lower C=O stretching frequencies would be expected to correlate with larger dihedral angles, in agreement with the observed trend. The detailed mechanism of the weakening, however, is less clear. Wiberg has discussed the complexities of the electronic structure of carbonyl groups as they relate to both the electronegativity of adjacent groups and the possibility of lone pair donation from adjacent heteroatom into π* orbitals of the carbonyl [36]. Either or both of these could contribute to the net charge on the carbonyl oxygens. Hyperconjugation may also play a role in some cases. Regardless of the mechanism, however, it is clear that for systems in the *cis* configuration, the average of the C=O stretching frequencies of the parent acids is a parameter through which the dihedral angles may be correlated. It is interesting to note that the one point that falls somewhat off the curve in Fig. 5 is the only one that involves a C_6H_5 substituent, suggesting the possibility of additional contributions from resonance structures that are enabled by the π system.

5. Conclusion

Jet-cooled microwave spectra of four carboxylic acid anhydrides, RCOOCOR′, have been measured and analyzed. For all systems studied, supporting computations predict nonplanar *cis* structures in which the two C=O groups are in the same general direction. Higher energy *trans* conformers are also predicted for all but pivalic trifluoroacetic anhydride. For systems with more than one predicted conformer, the calculated energy differences are small, typically less than 2 kcal/mol. Comparisons between experimental and calculated molecular constants indicate that nonplanar *cis* conformers were observed for four of the anhydrides studied in this work. Because of the low temperatures of the supersonic jet employed in this study, the observed *cis* conformers are assumed to represent the global potential energy minimum, in good agreement with the computed energies. A key structural feature in these systems is the through-space O=C···C=O dihedral angle. Variations in this angle are found to correlate with average of the carbonyl stretching frequencies of the two parent acids. The results of this study, combined with those of several others previously appearing in the literature, provide a new glimpse of the conformational complexity accessible to carboxylic acid anhydrides.

CRediT authorship contribution statement

Kenneth R. Leopold: Conceptualization, Project administration, Validation, Writing – review & editing, Supervision. **Nathan Love:** Conceptualization, Data curation, Formal Analysis, Investigation, Writing – Original Draft. **Aaron Reynolds:** Formal Analysis, Software Supervision, Validation, Writing- Review & editing. **Michael Dvorak:** Investigation, Writing – Review & editing.

Declaration of Competing Interest

The authors declare that they have no known competing financial interests or personal relationships that could have appeared to influence the work reported in this paper.

Data availability

Data will be made available on request.

Acknowledgements

This work was supported by the National Science Foundation (Grant No. CHE 1953528) and the Minnesota Supercomputing Institute. We thank Professor Steven Kass for a helpful discussion.

Appendix A. Supplementary data

Details of the synthesis of mixed anhydrides; Tables of observed transition frequencies, assignments, and residuals from the least squares fits; Tables of computed Cartesian coordinates. Supplementary data to this article can be found online at https://doi.org/10.1016/j.jms.2023.111844.

References

[1] See, for example, W. Caminati, J.-U. Grabow, Advancements in Microwave Spectroscopy, in Frontiers and Advances in Molecular Spectroscopy, Elsevier Inc, 2018, pp. 569–598 and references therein.
[2] See, for example, E.R. Alonso, I. León, J.L. Alonso, The Role of the Intramolecular Interactions in the Structural Behavior of Biomolecules: Insights from Rotational Spectroscopy, in Intra- and Intermolecular Interactions between Non-Covalently Bonded Species, E.R. Bernstein, Ed., Elsevier, Inc. 93-141 (2021) and references therein.
[3] In this paper, we refer to these systems as "carboxylic acid anhydrides" rather than the more familiar "acid anhydrides" in order to distinguish them from other types of anhydrides (e.g., carboxylic sulfuric anhydrides, which we have also studied extensively: C.J. Smith, A.K. Huff, K.R. Leopold, "Carboxylic Sulfuric Anhydrides", *J. Phys. Chem. A* 2020, 124, 601–612).
[4] A. Boogaard, H.J. Geise, F.C. Mijlhoff, An Electron Diffraction Investigation of the Molecular Structure of Formic Anhydride, J. Mol. Struct. 13 (1972) 53–58.
[5] S. Vaccani, A. Bauder, H. Hs, Günthard, Microwave Spectrum, Dipole Moment and Conformational of Formic Anhydride, Chem. Phys. Lett. 35 (1975) 457–460.
[6] S. Vaccani, U. Roos, A. Bauder, H. Hs, Günthard, Microwave Spectra, Substitution Structure and Vibrational Satellites of Formic Anhydride, Chem. Phys. 19 (1977) 51–57.
[7] G. Wu, S. Shlykov, C. Van Alsenoy, H.J. Geise, E. Sluyts, B.J. Van der Veken, Formic Anhydride in the Gas Phase, Studied by Electron Diffraction and Microwave and Infrared Spectroscopy, Supplemented with ab-Initio Calculations of Geometries and Force Fields, J. Phys. Chem. 99 (1995) 8589–8598.
[8] H.J. Vledder, F.C. Mijlhoff, F.P. Van Well, G.M.T. Dofferhoff, J.C. Leyte, An Electron Diffraction Investigation of the Molecular Structure of Formic Acetic Anhydride, J. Mol. Struct. 9 (1971) 25–32.

[9] G. Wu, S. Shlykov, C. Van Alsenoy, H.J. Geise, Formic Acetic Anhydride in the Gas Phase, Studied by Electron Diffraction and Infrared Spectroscopy, Supplemented with ab-Initio Calculations of Geometries and Force Fields, J. Phys. Chem.. 100 (1996) 11620–11629.
[10] A. Bauder, Microwave Spectrum of Formic Acetic Anhydride, Mol. Phys.. 111 (2013) 1999–2002.
[11] H.J. Vledder, F.C. Mijlhoff, J.C. Leyte, Vibrational Structure and Normal Coordinate Analysis of Formic Acetic Anhydride, J. Mol. Struct. 10 (1971) 57–73.
[12] H.J. Vledder, F.C. Mijlhoff, J.C. Leyte, C. Romers, An Electron Diffraction Investigation of the Molecular Structure of Gaseous Acetic Anhydride, J. Mol. Struct. 7 (1971) 421–429.
[13] G. Wu, C. Van Alsenoy, H.J. Geise, E. Sluyts, B.J. Van der Veken, I.F. Shishkov, L. V. Khristenko, Acetic Anhydride in the Gas Phase, Studied by Electron Diffraction and Infrared Spectroscopy, Supplemented With Ab Initio Calculations of Geometries and Force Fields, J. Phys. Chem. 104 (2000) 1576–1587.
[14] H.J. Vledder, F.S.M. Van Kleef, F.C. Mijlhoff, J.C. Leyte, Vibrational Spectra, Normal Coordinate Analysis, and Conformation of Acetic Anhydride, J. Mol. Struct. 10 (1971) 189–202.
[15] O.L. Stiefvater, The Complete Structure of Maleic Anhydride by DRM Microwave Spectroscopy, Z. Naturforsch. 33a (1978) 1480–1489, and references therein.
[16] A.M. Pejlovas, M. Sun, S.G. Kukolich, Microwave Measurements of the Spectra and Molecular Structure for Phthalic Anhydride, J. Mol. Spectrosc.. 299 (2014) 43–47.
[17] A.V. Belyakov, N. Vogt, J. Damaison, R.Y. Kulishenko, A.A. Oskorbin, Semiexperimental Equilibrium Molecular Structure of Phthalic Anhydride, Chem. Phys. Lett. 795 (2022), 139540.
[18] M.K. Jahn, D.A. Obenchain, K.P. Rajappan Nair, J.-U. Grabow, N. Vogt, J. Demaison, P.D. Godfrey, D. McNaughton, The Puzzling Hyper-fine Structure and an Accurate Equilibrium Geometry of Succinic Anhydride, PCCP 22 (2020) 5170–5177.
[19] N. Love, C.J. Smith, A.K. Huff, K.R. Leopold, A Microwave and Computational Study of Trifluoroacetic Anhydride, J. Mol. Spectrosc. 365 (2019), 111210.
[20] N. Love, A.K. Huff, K.R. Leopold, A New Program for the Assignment and Fitting of Dense Rotational Spectra Based on Spectral Progressions: Application to the Microwave Spectrum of Pivalic Anhydride, J. Mol. Spectrosc. 370 (2020), 111294.
[21] N. Love, Microwave Studies of Gas-Phase Molecules and Complexes: Automation, Structure, and Electronic Analysis, University of Minnesota, Minneapolis, MN, 2022. Ph.D. Thesis.
[22] S. Montiel-Smith, S. Meza-Reyes, O. Viñas-Bravo, M.A. Fernández-Herrera, R. Martínez-Pascual, J. Sandoval-Ramírez, A. Fuente, M. Reyes, J.A. Ruiz, *In Situ* Preparation of Mixed Anhydrides Containing the Trifluoroacetyl Moiety. Application to the Esterification of Cholesterol and Phenol, ARKIVOC 2005, Part vi., 127–135.
[23] B.E.J. Bourne, M. Stacey, J.C. Tatlow, R. Worrall, Studies of Trifluoroacetic Acid. Part XII. Acyl Trifluoroacetates and Their Reactions, J. Chem. Soc. (1954, 2006–2012.).
[24] R. Schijf, W. Stevens, Mixed Carboxylic Anhydrides VII. Synthesis of Some Mixed Formic Acid Anhydrides, Rec. Trav. Chim. Pays-Bas 85 (1966) 627–628.
[25] C.T. Dewberry, R.B. Mackenzie, S. Green, K.R. Leopold, 3D-Printed Slit Nozzles for Fourier Transform Microwave Spectroscopy, Rev. Sci. Instrum.. 86 (2015), 065107.
[26] J.A. Phillips, M. Canagaratna, H. Goodfriend, A. Grushow, J. Almlöf, K.R. Leopold, Microwave and ab initio investigation of HF-BF_3, J. Am. Chem. Soc. 117 (1995) 12549–12556.
[27] H.M. Pickett, The Fitting and Prediction of Vibration-Rotation Spectra with Spin Interactions, J. Mol. Spectrosc. 148 (1991) 371–377.
[28] H. Hartwig, H. Dreizler, The Microwave Spectrum of Trans-2,3-Dimethyloxirane in Torsional Excited States, Z. Naturforsch. Phys. Sci. 51a (1996) 923–932.
[29] J. Kraitchman, Determination of Molecular Structure from Microwave Spectroscopic Data, Am. J. Phys 21 (1953) 17–24.
[30] The KRA Program, Written by Z. Kisiel, may be downloaded from www.Ifpan.Edu.Pl/~kisiel/Struct/Struct.Htm#kra.
[31] Gaussian 16, Revision C.01, M.J. Frisch, G.W. Trucks, H.B. Schlegel, G.E. Scuseria, M.A. Robb, J.R. Cheeseman, G. Scalmani, V. Barone, G.A. Petersson, H. Nakatsuji, X. Li, M. Caricato, et al., Gaussian, Inc., Wallingford CT, 2016.
[32] R.E. Asfin, IR Spectra of Hydrogen-Bonded Complexes of Trifluoroacetic Acid with Acetone and Diethyl Ether in the Gas Phase. Interaction between CH and OH Stretching Vibrations, Chem. A Eur. J. 123 (2019) 3285–3292.
[33] J.M. Bakker, L.M. Aleese, G. von Helden, G. Meijer, The Infrared Absorption Spectrum of the Gas Phase Neutral Benzoic Acid Monomer and Dimer, J. Chem. Phys. 119 (2003) 11180.
[34] K.A.E. Meyer, M.A. Suhm, Vibrational Exciton Coupling in Homo and Hetero Dimers of Carboxylic Acids Studied by Linear Infrared and Raman Jet Spectroscopy, J. Chem. Phys. 149 (2018), 104307.
[35] J.K. Wilmshurst, Infrared Investigation of Acetic Acid and Acetic Acid – d Vapors and a Vibrational Assignment of the Monomeric Acids, J. Chem. Phys. 25 (1956) 1171–1173.
[36] K.B. Wiberg, The Role of Electrostatic Effects in Organic Chemistry, J. Chem. Ed. 73 (1996) 1089–1095.